Comparative Analysis of Spectral Feature Fitting (SFF) and Spectral Angle Mapper (SAM) in the Delineation of Hydrothermally Altered Mineral in Jahazpur, Rajasthan, India using AVIRIS-NG Hyperspectral Data

Gaurav Mishra (1), Himanshu Govil (1), Mahesh Kumar Tripathi (1), Subhanil Guha (1), Monika (1), Arjun Pratap Shahi (1)
[1] Department of Applied Geology, National Institute of Technology Raipur- 492010, Chhattisgarh, India
Email: mshgaurav04@gmail.com; hgovil.geo@nitrr.ac.in; TRIPATHI.MAHESH1@gmail.com; subhanilguha@gmail.com; geniousmonika11@gmail.com; arjunpratapshahi@gmail.com

KEY WORDS: hyperspectral, remote sensing, spectral signature, clay minerals

ABSTRACT: Hyperspectral remote sensing techniques is considered as robust techniques for the identification and delineation of altered mineral deposits. The purpose of this study is to compare the classified map of hydrothermally altered rocks in Jahazpur area, Rajasthan, India using spectral feature fitting (SFF) and spectral angle mapper (SAM) algorithms. The method is based on the comparison of absorption features in the image with the reference spectra. The Jahazpur belt is dominated by the occurrence of phyllite, dolomite, quartzite, limonite/goethite in folded sequence and affected by low grade greenschist facies of metamorphism. Hydrothermal alteration zones are delineated based on Airborne Visible/Infrared imaging spectrometer- Next Generation (AVIRIS-NG) remote sensing data. In the first stage, atmospheric correction was performed followed by minimum noise fraction, pixel purity index. Spectral signature of different minerals such as Kaosmec, Talc, Kaolinite, Dolomite and montmorillonite were derived in SWIR (Shortwave infrared) region while Iron oxides such as Goethite and limonite were distinguished in the VNIR (Visible and Near Infrared) region of electromagnetic spectrum. Then image classification techniques such as spectral angle mapper (SAM) and spectral feature fitting (SFF) methods were used. SAM algorithm used for the surface mineral mapping with reference mineral spectra using USGS spectral library. The threshold values for talc, mixture of iron and talc, kaosmec, limonite/goethite are 0.08, 0.07, 0.08, 0.08 radians respectively. The classified image successfully shows the occurrence of these minerals in distribution map. SFF algorithm classified the same minerals and mapped at the default threshold (30 for all) value. The SFF distribution map shows the occurrence of clay minerals such as kaolinite, talc, and goethite. Comparatively, SFF shows better result for the mapping of clay mineral in river channel and shows cluster of pixels at the talc deposit whereas SAM shows clear distinct boundary around talc deposit. Therefore, it is concluded that spectral angle mapper produces better classified map of altered minerals than spectral feature fitting for AVIRIR-NG data.

1. Introduction

Remote sensing is the science of acquiring, processing and interpretating images and related data, acquired from aircraft and satellites which records the interaction between matter and electromagnetic energy (Sabins, 1999). The combination of remote sensing and spectroscopy is known as imaging spectroscopy or hyperspectral remote sensing (Goetz et al., 1985). The use of multispectral remote sensing was limited in the identification and delineation of minerals due to wide spectral resolution. But with the development of hyperspectral remote sensing, the

identification, delineation and mapping of earth surface features is easily possible due narrow spectral resolution of the data (R. N Clark, 1999). The visible and near infrared (VNIR) to Shortwave infrared (SWIR) range is useful in the identification of minerals because of characteristic absorption feature at particular wavelength (F. A. Kruse et al., 1993a; Cudahy et al., 2002; Fred A. Kruse, Boardman, & Huntington, 2003a; Farooq & Govil, 2014; Govil et al., 2018).

Hydrothermal alteration processes produce physico-chemical changes in the rocks through which they circulate. When the hydrothermal fluid comes in contact with the wall rock, a number of chemical reactions have been taken place and processes of dissolution and precipitation produce new mineral assemblages. The nature and type of hydrothermal alteration depends upon pressure, temperature and chemistry of circulating fluid as well as nature and composition of the rocks through which the fluid circulates.

Hyperspectral remote sensing utilizes reflectance spectral signature of an object in narrow and contiguous spectral band and overcomes the limitations of multispectral remote sensing for identifying mineral and rocks accurately (Goetz, 2009). Hyperspectral remote sensing utilizes the fact that each mineral has, depending on structure and chemistry of crystal lattice, its characteristic spectral absorption feature in the identification of mineral and mineral aggregates (Graham R. Hunt & Salisbury, 1970; G. R. Hunt & Ashley, 1979; Goetz et al., 1985; Burns, 1993; Goetz, 2009; Rossman, 2019). Laboratory, field, airborne and spaceborne measurements of spectral signatures have proved to be useful in various fields of applications related to geology, such as lithologic mapping (Roger N. Clark, Swayze, & Gallagher, 1992; Roger N Clark, 1995; F. van der Meer, Vazquez-Torres, & van Dijk, 1997; Rowan, Simpson, & Mars, 2004) and mineral exploration (F. A. Kruse et al., 1993b; Bierwirth, 2002; Swayze et al., 2004) and hydrothermal alteration mineral mapping (Bierwirth, 2002; F A Kruse et al., 2002; Fred A. Kruse, Boardman, & Huntington, 2003b; Kennedy-Bowdoin et al., 2004; Fred A. Kruse, Perry, & Caballero, 2006; AJ Brown, 2010).

Airborne Visible InfraRed Imaging Spectrometer - Next Generation (AVIRIS-NG) is the airborne sensor and data us acquired in the range of 380 - 2510nm with the spectral resolution of 5nm. Airborne sensors also provide a high resolution data for various scientific domains (F A Kruse et al., 2002). The narrow spectral resolution allows to identify the basic surface mineralogy. Mineral mapped by using AVIRIS-NG include clay minerals, hydroxyl-bearing minerals, carbonates etc (Roger N. Clark et al., 2006).

The matching of spectral features similarity between unknown mineral (pixel) spectral and predefined spectra from mineral spectral library formed the basis of delineation of mineral boundary at ground (Freek Van Der Meer et al., 2003). Present study compares the image analysis and processing methods such as spectral feature fitting (SFF) and spectral angle mapper (SAM) in the identification of minerals. The classified images by spectral angle mapper (SAM) and spectral feature fitting (SFF) have been compared with the lithology of the area and generated the mineral delineation map.

2. Study area

The study area is located in Jahazpur town of Bhilwara district in Rajasthan, India. The area is in south-eastern part of the Jahazpur city. The NE-SW trending Jahazpur belt is stretched linearly and pinching out at the end. The Jahazpur belt is divided into two sub belts namely, Eastern Jahazpur Belt and Western Jahazpur Belt (Malhotra & Pandit, 2000). The Eastern Jahazpur belt extends from Khorpur in the SW to Naenwa in NE and Western Jahazpur belt

extends from Jawal in SW to Dhandola in NE. The linear stretch of Western Jahazpur belt is 60km whereas Eastern Jahazpur belt extends up to 90km. The Jahazpur belt is dominated by the presence of metasedimentary rock along the eastern fringe of Aravalli carton. The rocks have been metamorphosed by low grade greenschist facies of metamorphism and rest over Archean basement.

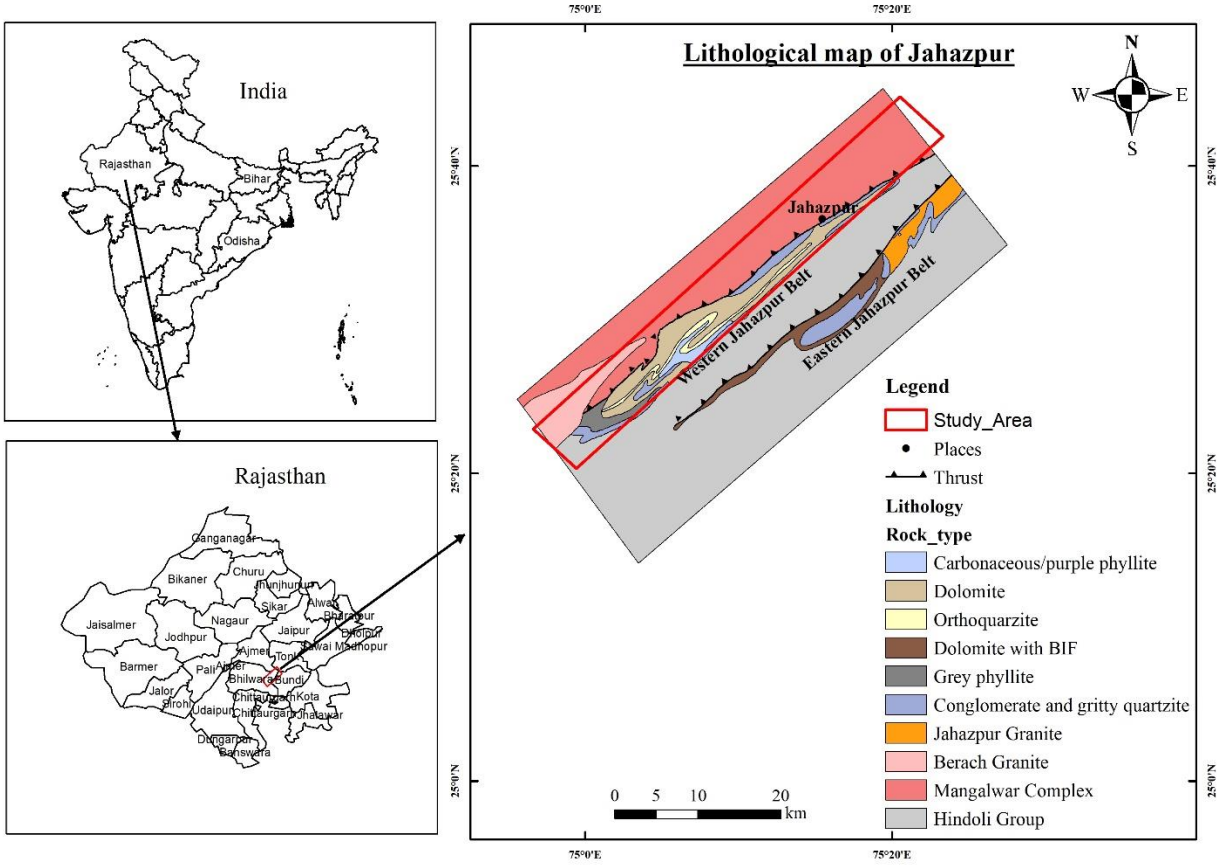

Figure 1. Geological map of the study area with different rock type near Jahazpur, Bhilwara district, Rajasthan (Modified after Pandit et al. 2003)

The stratigraphy of the study area is described in the following Table 1.

Table 1: Stratigraphy of the study area and associated lithologies (Malhotra & Pandit, 2000).

Group	Formation	Mineralogy
Jahazpur Group	Carbonaceous Phyllite	Sericite, quartz
	Dolomite	Dolomite
	Orthoquartzite	Quartz
	Dolomite with BIF	Dolomite, hematite, magnetite
	Grey Phyllite	Calcareous, Mica, quartz, chlorite
	Conglomerate/gritty quartzite	Jointed & fragmented quartzite, quartz, feldspar
----------Unconformity----------		
Hindoli Group	Upper Hindoli	Turbidites, metagraywackes, phyllites, schist
	Lower Hindoli	Bimodal volcanics
----------Unconformity----------		

3. Materials and method

The overall methodology, algorithm and processing steps have been shown in the figure 2.

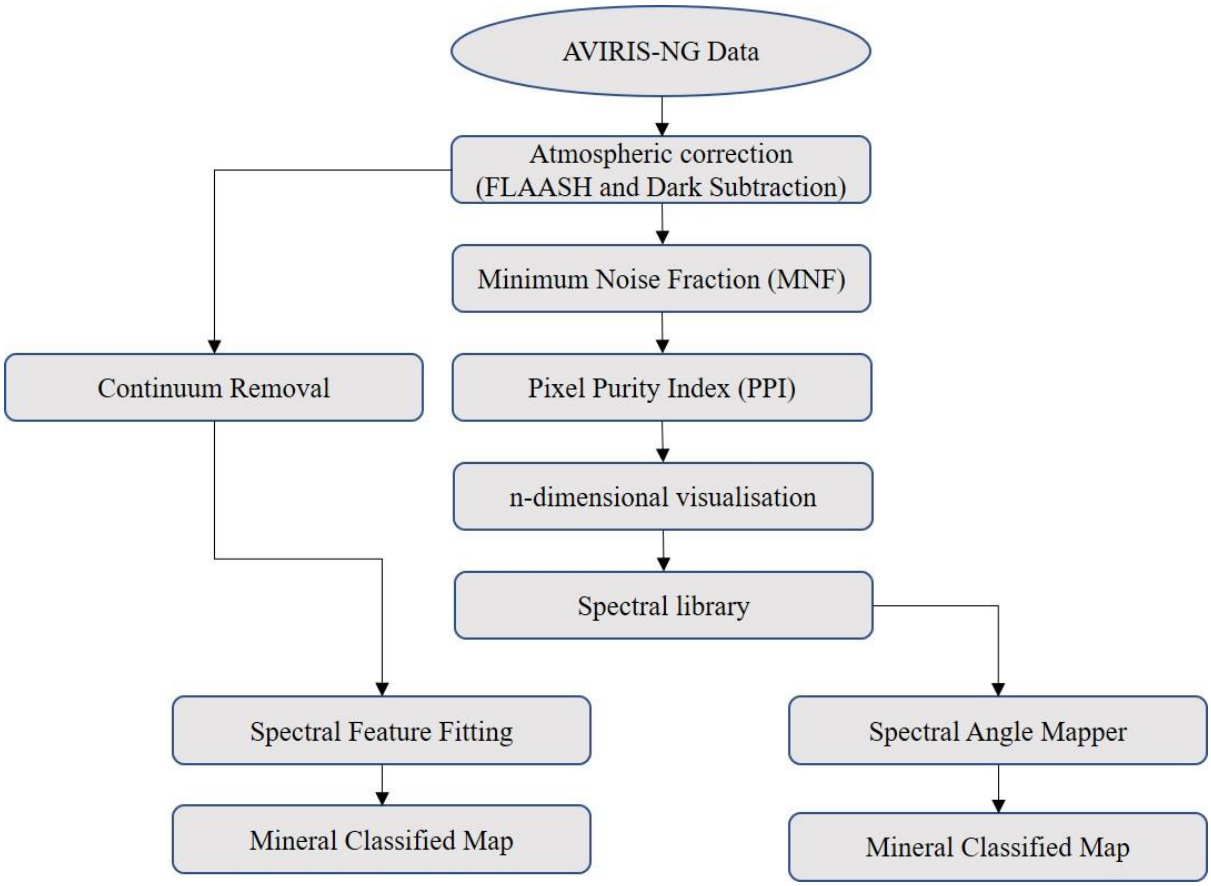

Figure 2. Flow chart showing the methodology of hyperspectral data processing and mineral classification using spectral angle mapper (SAM) and spectral feature fitting (SFF).

3.1 Atmospheric correction

The AVIRIS-NG sensor acquires radiance energy which is reflected from the earth surface. To convert the radiance into reflectance, atmospheric correction has been applied. The FLAASH atmospheric correction algorithm corrects the image for haze, noise, water vapour and gases present in the atmosphere.

3.2 Minimum Noise Fraction

Minimum noise fraction reduces the dimensionality in the data. The conversion of high dimensional data into low dimensional data without losing the information is known as dimensionality reduction. To enhance the analytical accuracy, dimensionality reduction is the necessary process. MNF successfully reduce the dimensionality of the datasets on the basis of noise statistics information and eliminated the noise. Nearest neighbour method is used for the computation of the noise statistics given by (Green et al., 1988).

3.3 Pixel Purity Index

Pixel purity index is applied to MNF to extract the purest pixels. PPI is used for the extraction of endmembers hyperspectral data. The extreme pixels have been selected from region of interest (ROI). Extraction of pure pixel and evaluation of their spectra, the n-dimensional visualisation method applied to ROI on MNF image.

3.4 Spectral Angle Mapper (SAM)

Spectral angle mapper (SAM) is a supervised classification technique which compare the image spectra and reference spectra collected from spectral library (Cŕosta et al., 2003). The algorithm for SAM classification is based on angle between image spectra and the reference spectra in n-dimensional vector space. The similarity between the image and reference spectra depends on the angle between spectrums such as high angle shows less similarity and less angle shows high similarity.

The spectral angle can have values between 0 and π/2 and is calculated from the formula given by (F. A. Kruse et al., 1993a):

$$\theta = cos^{-1}\left[\frac{\sum_{i=1}^{n} t_i r_i}{\sqrt{\sum_{i=1}^{n} t_i^2 \sum_{i=1}^{n} r_i^2}}\right]$$

where

n = the number of spectral bands

t = the reflectance of the actual spectrum and

r = the reflectance of the reference spectrum

3.5 Spectral Feature Fitting (SFF)

Spectral feature fitting (SFF) algorithm removes the continuum of absorption feature from the image spectra and library spectra. Spectral feature fitting compares the continuum removed image spectra with the reference spectral library spectra after continuum removal process and operated the least square fitting. The identification of best fitting material depends on spectral features of reference and done by comparing the correlation coefficient of fits (Boardman & Kruse, 1994). Continuum removed image spectra can be derived by dividing the original spectrum of every pixel in an image from continuum curve.

$$s_{cr} = \frac{s}{c}$$

Where

S_{cr} = Continuum removed spectra

S = Original Spectra

C = Continuum curve

Scale factor represents the abundance of spectral features. Band by band calculation is performed for computation of least square fit. The greater scale value represents the strong

absorption in mineral spectra and the abundance of mineral is highly related to the scale value (Freek van der Meer, 2004). Scale image with brighter pixels displays good matching of pixel spectrum with reference spectrum of mineral. RMS (Root Mean Square) error image is also produced for each endmember to compute the total RMS error. The low RMS error and high scale factors are closely matched pixels. An equal number of images are generated by the scale and RMS. The fit images are generated by ratio between scale image and RMS error image to measure the similarities between the unknown spectrum and reference spectrum on the basis of pixel-by-pixel (Freek Van Der Meer et al., 2003).

4. Result and Discussion

Ghevariya is the well-known deposit of talc and it shows the absorption feature at 2.31µm with doublet at 2.28 µm dur to absorption features of Mg-OH. The goethite/limonite are found in the dolomitic rock and shows characteristic absorption feature at 0.54µm and 0.92µm due to electronic absorption. Montmorillonite shows distinct absorption features at 2.20 µm due to presence of Al-OH. Goethite/limonite, talc, montmorillonite spectra have been collected from end-member collection and spectral angle mapper and spectral feature fitting used for the identification of minerals. The classified image by SAM and SFF have been compared with the lithological map of the area.

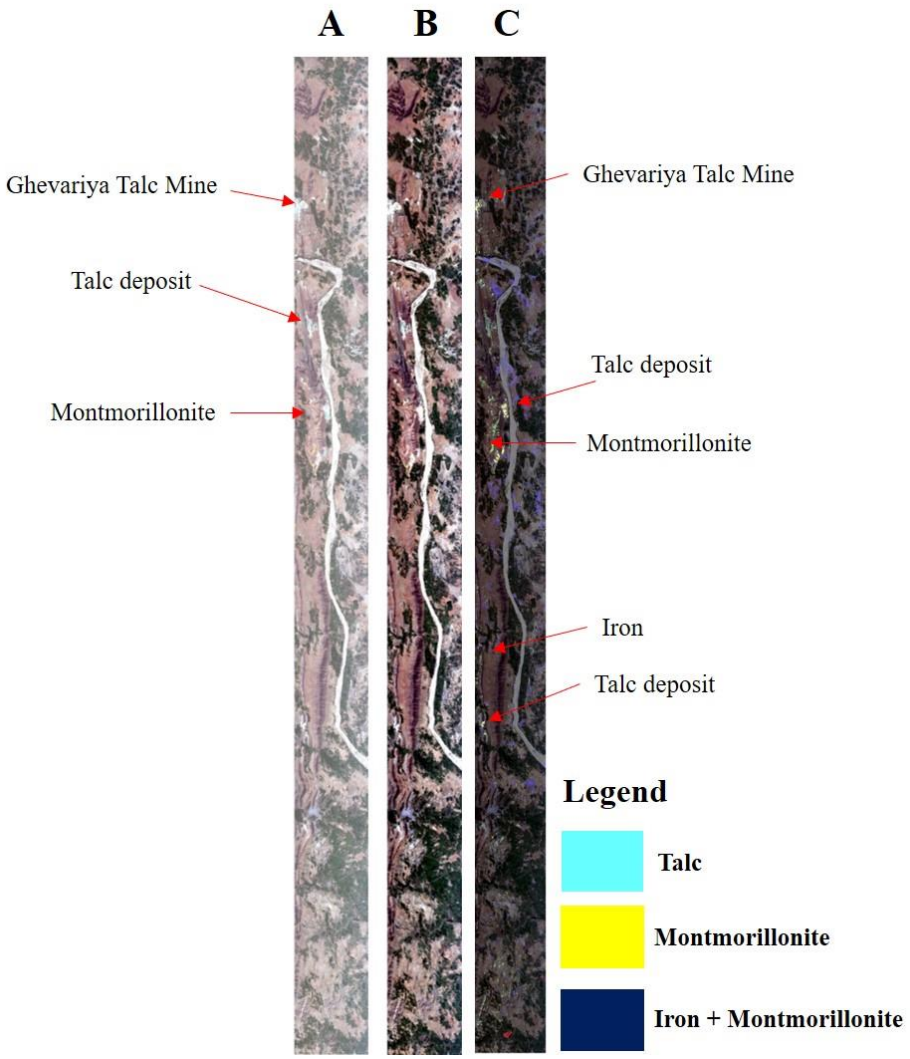

Figure. 3. A). SAM classified image; B) AVIRIS-NG scene; and C) SFF classified image for mineral distribution.

5. Conclusion

Clay mineral (montmorillonite, talc) and iron oxides (goethite, limonite) are the common mineral present in the study area affected by hydrothermal alteration. Mining area such as Ghevariya Talc mine are clearly delineated using spectral angle mapper. The surface exposure of talc due to open cast mine facilitated the mapping of talc using image classification techniques such as SAM and SFF. Spectral angle mapper classifies the map very clearly for talc, montmorillonite and iron minerals whereas Spectral feature fitting is more useful to delineate the montmorillonite presence in the stream bed. Comparatively, SFF shows better result for the mapping of clay mineral and iron in and around river channel and shows cluster of pixels at the talc deposit whereas SAM shows clear distinct boundary around talc deposit.

References

AJ Brown, S. H. A. B. J. C. N. B. B. T. G. M. F. S. J. B., 2010. Hydrothermal formation of clay-carbonate alteration assemblages in the Nili Fossae region of Mars, Earth planet. Sci Lett, 297, pp. 174–182.

Bierwirth, P., 2002. Hyperspectral Mapping of Mineral Assemblages Associated with Gold Mineralization in the Central Pilbara, Western Australia. Economic Geology.

Boardman, J. W., & Kruse, F. A., 1994. Automated spectral analysis: a geological example using AVIRIS data, north Grapevine Mountains, Nevada. Proceedings of the Thematic Conference on Geologic Remote Sensing.

Burns, R. G., 1993. Mineralogical applications of crystal field theory. Second edition. Mineralogical applications of crystal field theory. Second edition.

Clark, R. N., 1999. Spectroscopy of rocks andminerals, and principles of spectrocopy. Remote sensing for the earth sciences: Manual of remote sensing.

Clark, Roger N., Boardman, J., Mustard, J., Kruse, F., Ong, C., Pieters, C., & Swayze, G. A., 2006. Mineral mapping and applications of imaging spectroscopy. In: International Geoscience and Remote Sensing Symposium (IGARSS).

Clark, Roger N., Swayze, G. A., & Gallagher, A., 1992. Mapping the mineralogy and lithology of Canyonlands, Utah with imaging spectrometer data and the multiple spectral feature mapping algorithm. In: Summaries of the Third Annual JPL Airborne Geoscience Workshop. Volume 1: AVIRIS Workshop.

Clark, Roger N., 1995. Mapping minerals, amorphous materials, environmental materials, vegetation, water, ice and snow, and other materials: The USGS tricorder algorithm. Clark, Roger N. SwaySummaries of the Fifth Annual JPL Airborne Earth Science Workshop. Volume 1: AVIRIS Workshopze, Gregg A.

Cŕosta, A. P., De Souza Filho, C. R., Azevedo, F., & Brodie, C., 2003. Targeting key alteration minerals in epithermal deposits in Patagonia, Argentina, using ASTER imagery and principal component analysis. International Journal of Remote Sensing, 24, pp. 4233–4240.

Cudahy, T. J., Rodger, A. P., Barry, P. S., Mason, P., Quigley, M., Folkman, M., & Pearlman, J., 2002. Assessment of the stability of the Hyperion SWIR module for hyperspectral mineral mapping using multi-date images from Mount Fitton, Australia. In: International Geoscience and Remote Sensing Symposium (IGARSS).

Farooq, S., & Govil, H., 2014. Mapping Regolith and Gossan for Mineral Exploration in the

Eastern Kumaon Himalaya, India using hyperion data and object oriented image classification. Advances in Space Research.

Goetz, A. F. H., 2009. Three decades of hyperspectral remote sensing of the Earth: A personal view. Remote Sensing of Environment.

Goetz, A. F. H., Vane, G., Solomon, J. E., & Rock, B. N., 1985. Imaging spectrometry for earth remote sensing. Science.

Govil, H., Gill, N., Rajendran, S., Santosh, M., & Kumar, S., 2018. Identification of new base metal mineralization in Kumaon Himalaya, India, using hyperspectral remote sensing and hydrothermal alteration. Ore Geology Reviews, 92, pp. 271–283.

Green, A. A., Berman, M., Switzer, P., & Craig, M. D., 1988. A Transformation for Ordering Multispectral Data in Terms of Image Quality with Implications for Noise Removal. IEEE Transactions on Geoscience and Remote Sensing.

Hunt, G. R., & Ashley, R. P., 1979. Spectra of altered rocks in the visible and near infrared. Economic Geology, 74, pp. 1613–1629.

Hunt, Graham R., & Salisbury, J. W., 1970. Visible and near-infrared spectra of minerals and rocks: 1. Silicate minerals. Modern Geology.

Kennedy-Bowdoin, T., Silver, E. A., Martini, B. A., & Pickles, W. L., 2004. Geothermal prospecting using hyperspectral imaging and field observations, Dixie Meadows, NV. In: Transactions - Geothermal Resources Council.

Kruse, F. A., Lefkoff, A. B., Boardman, J. W., Heidebrecht, K. B., Shapiro, A. T., Barloon, P. J., & Goetz, A. F. H., 1993a. The spectral image processing system (SIPS)-interactive visualization and analysis of imaging spectrometer data. Remote Sensing of Environment, 44, pp. 145–163.

Kruse, F. A., Lefkoff, A. B., Boardman, J. W., Heidebrecht, K. B., Shapiro, A. T., Barloon, P. J., & Goetz, A. F. H., 1993b. The spectral image processing system (SIPS)-interactive visualization and analysis of imaging spectrometer data. Remote Sensing of Environment.

Kruse, F A, Imaging, A., Huntington, F., Ryde, N., & Team, V., 2002. Comparison of EO-1 Hyperion and Airborne Hyperspectral Remote Sensing Data for Geologic Applications, pp. 1501–1513.

Kruse, Fred A., Boardman, J. W., & Huntington, J. F., 2003a. Comparison of airborne hyperspectral data and EO-1 Hyperion for mineral mapping. IEEE Transactions on Geoscience and Remote Sensing, 41, pp. 1388–1400.

Kruse, Fred A., Boardman, J. W., & Huntington, J. F., 2003b. Comparison of airborne hyperspectral data and EO-1 Hyperion for mineral mapping. IEEE Transactions on Geoscience and Remote Sensing.

Kruse, Fred A., Perry, S. L., & Caballero, A., 2006. District-level mineral survey using airborne hyperspectral data, Los Menucos, Argentina. Annals of Geophysics.

Malhotra, G., & Pandit, M. K., 2000. Geology and mineralization of the Jahazpur Belt, southeastern Rajasthan. Narosa Publishing.

Meer, Freek Van Der, Jong, S. De, van der Meer, F. D., & de Jong, S. J., 2003. Spectral

mapping methods: many problems, some solutions. 3rd EARSeL workshop on imaging spectroscopy.

Pandit, M. K., Sial, A. N., Malhotra, G., Shekhawat, L. S., & Ferreira, V. P., 2003. C-, O-isotope and whole-rock geochemistry of proterozoic Jahazpur carbonates, NW Indian Craton. Gondwana Research, 6, pp. 513–522.

Rossman, G. R., 2019. Vibrational spectroscopy of hydrous components. In: Spectroscopic Methods in Mineralogy and Geology.

Rowan, L. C., Simpson, C. J., & Mars, J. C., 2004. Hyperspectral analysis of the ultramafic complex and adjacent lithologies at Mordor, NT, Australia. Remote Sensing of Environment.

Sabins, F. F., 1999. Remote sensing for mineral exploration. Ore Geology Reviews, 14, pp. 157–183.

Swayze, G. A., Higgins, C. T., Clinkenbeard, J. P., & Kokaly, R. F., 2004. Preliminary Report on Using Imaging Spectroscopy to Map Ultramafic Rocks , Serpentinites , and Tremolite-Actinolite-Bearing Rocks in California. California Geological Survey.

van der Meer, F., Vazquez-Torres, M., & van Dijk, P. M., 1997. Spectral characterization of ophiolite lithologies in the troodos ophiolite complex of cyprus and its potential in prospecting for massive sulphide deposits. International Journal of Remote Sensing.

van der Meer, Freek., 2004. Analysis of spectral absorption features in hyperspectral imagery. International Journal of Applied Earth Observation and Geoinformation.